OZSpeech: One-step Zero-shot Speech Synthesis with Learned-Prior-Conditioned Flow Matching

Anonymous ACL submission

Abstract

Text-to-speech (TTS) systems have seen significant advancements in recent years, driven by improvements in deep learning and network architectures. Viewing the output speech as a data distribution, previous approaches often employ traditional speech representations, such as waveforms or spectrograms, within the Flow Matching framework. However, these methods have limitations, including overlooking various speech attributes and incurring high computational costs due to additional constraints introduced during training. To address these challenges, we introduce *OZSpeech*, the first TTS method to explore optimal transport conditional flow matching with one-step sampling and a learned prior as the condition, effectively disregarding preceding states and reducing the number of sampling steps. Our approach operates on disentangled, factorized components of speech in token format, enabling accurate modeling of each speech attribute, which enhances the TTS system's ability to precisely clone the prompt speech. Experimental results show that our method achieves promising performance over existing methods in content accuracy, naturalness, prosody generation, and speaker style preservation. Code and audio samples are available at our demo page [1].

1 Introduction

Text-to-speech (TTS) has numerous real-world applications, such as voice-based virtual assistants, assistive screen readers for the visually impaired, and reading aids for people with dyslexia, to name a few. Most TTS systems focus on synthesizing speech that matches a speaker in a set of speakers seen during training. Recent studies tackle a more challenging problem of converting text into speech that follows the acoustic characteristics of a prompt spoken by a speaker not seen during training. This problem is called zero-shot TTS.

[1] https://ozspeech.github.io/OZSpeech_Web/

In recent years, remarkable progress has been achieved in the research of Zero-shot TTS models. These advancements have demonstrated the impressive capabilities of such models, with their synthesized outputs often approaching a quality level that is virtually indistinguishable from human speech. The body of research on Zero-Shot TTS can be broadly divided into two primary categories, each aligned with a dominant methodological paradigm in the field: autoregressive models and diffusion-based models.

Prominent examples of the autoregressive approach are VALL-E (Chen et al., 2025) and its variants (Chen et al., 2024a; Zhang et al., 2023; Han et al., 2024; Meng et al., 2024; Song et al., 2024; Peng et al., 2024; Ji et al., 2024a), which have significantly advanced Zero-Shot TTS by integrating language modeling techniques and employing disentangled speech units as input and output tokens. This innovative framework has paved the way for the potential convergence of Zero-Shot TTS with large language models (LLMs), enabling the creation of efficient, multimodal systems which are capable of generating text, speech, and other modalities in a flexible and scalable manner. However, as with other LLM-based systems, autoregressive models are susceptible to the issue of the non-deterministic sampling process, potentially leading to infinite repetition, which remains a critical challenge in applications requiring high levels of precision and reliability.

In contrast, diffusion-based models, as demonstrated by state-of-the-art (SOTA) TTS systems such as E2 TTS (Eskimez et al., 2024) and other related approaches (Le et al., 2023; Vyas et al., 2023; Shen et al., 2024; Ju et al., 2024b), have emerged as powerful generative frameworks capable of producing high-quality, natural-sounding audio. This approach has proven particularly effective in specialized tasks such as in-filling and speech editing. Nevertheless, diffusion-based mod-

els face limitations in real-time applications due to the computational inefficiency of their multi-step sampling processes. These constraints underscore the trade-offs inherent in the diffusion-based paradigm, particularly in scenarios that demand low-latency performance.

Distillation methods for diffusion-based models have been explored to address the multi-step sampling challenge, with Consistency Models (Song et al., 2023) introducing one-to-one mapping functions that transform intermediate states along the Ordinary Differential Equation (ODE) trajectory directly to their origin. This approach reduces sampling steps to one while maintaining output quality but requires access to a full range of $t \in [0, 1]$ to approximate trajectories, demanding extensive training steps. As an alternative, Shortcut Models (Frans et al., 2024) condition the network on noise level and step size, enabling faster generation with fewer training steps by using only a subset of t values. However, this method is computationally intensive due to additional constraints introduced during training, making it more resource-demanding than Consistency Models.

To capitalize on the strengths and mitigate the limitations of the aforementioned approaches, we propose OZSpeech (**O**ne-step **Z**ero-shot **Speech** Synthesis with Learned-Prior-Conditioned Flow Matching), a novel Zero-Shot TTS system. Our model leverages optimal transport conditional flow matching (Lipman et al., 2023) (OT-CFM), a class of diffusion-based models. We reformulate the original OT-CFM to enable single-step sampling, where the vector field estimator regresses the trajectories of all pairs of initial points from the learned prior distribution, rather than conventional Gaussian noise, to their respective target distributions. By minimizing the distance between the initial points and their origins while implicitly learning the optimal t for each prior, this approach eliminates the need to access a comprehensive range of t values or compute additional constraints, thereby ensuring high-fidelity synthesized speech.

The key contributions of this paper are as follows:

- We propose a reformulated OT-CFM framework that effectively initializes the starting points of the flow matching process using samples from a learned prior distribution. This prior is optimized to closely approximate the target distribution, enabling one-step sampling with minimal errors. Our framework requires only a single training run without the need for an extensive distillation stage.
- We propose a simple yet effective network architecture to learn prior-distributed codes.
- Compared to previous methods, our model yields multi-fold improvement in WER and latency, achieving significant reduction in model size while striking a balance with acoustical quality. In addition, while previous models suffer from increasing noise level in the audio prompts, OZSpeech's WER remains stable, highlighting the excellent noise-tolerant intelligibility of our method. Our model requires significantly less computation, with inference speed being $2.7 - 6.5$ times faster than the other methods. Our model is only 29%-71% the size of the other models.

2 Related Work

Zero-Shot TTS enables the generation of speech in an unseen speaker's voice using only a few seconds of audio as a prompt; this process is often termed voice mimicking. Advances in large-scale generative models have driven significant progress in this field. One prominent development is the adoption of diffusion models (Ho et al., 2020; Song et al., 2021), which have demonstrated remarkable performance (Kang et al., 2023; Tran et al., 2023; Shen et al., 2024; Ju et al., 2024b). Another approach, flow matching (Lipman et al., 2023; Liu et al., 2023), has further advanced the state-of-the-art by delivering strong results with reduced inference times (Kim et al., 2023; Mehta et al., 2024; Eskimez et al., 2024; Chen et al., 2024c). Additionally, a key innovation in Zero-Shot TTS is the use of discrete tokens, often derived from neural codecs (Wang et al., 2023; Kharitonov et al., 2023; Chen et al., 2024b; Ju et al., 2024a; Du et al., 2024a).

Neural codecs are designed to learn discrete speech and audio tokens, often referred to as acoustic tokens, while preserving reconstruction quality and maintaining a low bitrate. SoundStream (Zeghidour et al., 2022) is a well-known example that employs a vector-quantized variational autoencoder (VQ-VAE), which was first introduced by (van den Oord et al., 2017) in the field of computer vision, and later adapted to TTS, to disentangle continuous data into discrete tokens. It comprises multiple residual vector quantizers to compress speech into multiple tokens, which serve as intermediate representations for speech generation. A significant

breakthrough in this area, inspired by the success of LLMs in natural language processing, is VALL-E (Chen et al., 2025), a pioneering work in this domain. VALL-E represents speech as discrete codec codes using an off-the-shelf neural codec and redefines TTS as a conditional codec language modeling task. This approach has sparked further research and development in the field (Kharitonov et al., 2023; Zhang et al., 2023; Chen et al., 2024a; Han et al., 2024; Du et al., 2024b).

3 Method

3.1 Problem Statement

In this paper, we consider the problem of generating speech from given text and acoustic prompt such that conditions for the outputs are met. Viewing the synthesized speech as a data distribution, denoted as $\mathrm{x}_1 \sim p_1(x)$, previous methods often construct the output data distribution from a noise distribution $\mathrm{x}_0 \sim p_0(x)$. However, we propose constructing the output data distribution from a feasible intermediate state candidate $\mathrm{x}_{\text{pr}} \sim p_{\text{prior}}(x)$ instead of x_0, thereby disregarding preceding states and reducing the number of sampling steps. To achieve this, we undertake the following steps:

- **Prior Code Generation:** We design an effective method for generating prior codes to produce $\mathbf{x}_{\text{pr}}$ (see Section 3.2).
- **Vector Field Estimation:** We develop a vector field estimator to approximate v_θ , facilitating the transition from x_{pr} to x_1 (see Section 3.3).
- **Waveform Decomposition via FACodec:** We employ FACodec (Ju et al., 2024b), a neural codec disentangler framework, to decompose the waveform into distinct components, including speaker identity and sequences of codes encoding prosody, content, and acoustic details. This decomposition enables precise control over the aspects of speech to be preserved or modified.

3.2 Prior Codes Generation Modeling

Our key contribution to prior code generation is that the process follows a hierarchical structure: each code sequence generation depends on the preceding code sequences, while the condition for the first code sequence is initialized based on phoneme embeddings. To achieve this, we implement a cascaded neural network where specific decoder layers generate the respective code sequences in the hierarchy (shown in Fig. 1b). Formally, the Prior Codes Generator $\mathbf{f}_\psi(\cdot)$ is modeled as:

$$p(\mathbf{q}_{1:6} \mid \mathbf{p}; \psi) = p(\mathbf{q}_1 \mid \mathbf{p}; f_\psi^1) \prod_{j=2}^{6} p(\mathbf{q}_j \mid \mathbf{q}_{j-1}; f_\psi^j), \tag{1}$$

where $\mathbf{q}_j$ is the j-th code sequence from the Feed-Forward Transformer (FFT) decoder layer f_ψ^j and $\mathbf{p}$ represents phoneme embeddings as the initial condition. The Prior Loss $\mathcal{L}_{\text{prior}}$ minimizes the negative logarithm of the joint probability in Eq. (1), ensuring content code sequences are learned effectively by conditioning on phonemes, while the others, including prosody and acoustic details, converge towards the mean representations. The Prior Codes Generator produces semantically meaningful codes, reducing the distance between $\mathbf{x}_{\text{pr}}$ and $\mathbf{x}_1$, allowing the Vector Field Estimator $\mathbf{v}_\theta(\cdot, \cdot)$ to approximate vectors from a mean distribution rather than generating them from pure noise.

To align the input phonemes with their corresponding output code sequences, we employ a neural network functioning as a Duration Predictor, as introduced in (Ren et al., 2019a). Briefly, the Duration Predictor estimates the duration (i.e., the number of acoustic tokens) for each input phoneme. The phoneme embeddings are duplicated accordingly before being passed through the decoder of the Prior Codes Generator. We define the loss function used to train the Duration Predictor as $\mathcal{L}_{dur}$, which aims to minimize the mean squared error between the predicted and ground truth durations on a logarithmic scale.

3.3 One-Step Optimal Transport Flow Matching for Zero-Shot TTS

One-Step Optimal Transport Flow Matching Formulation. We rectify the OT-CFM paradigm, simultaneously introduced by (Lipman et al., 2023) and (Liu et al., 2023) and first adapted to text generation by (Hu et al., 2024). Our approach involves constructing a vector field that regresses the velocity of non-Gaussian distribution and data distribution pairs, where the initial distribution closely approximates the target distribution. To this end, we reformulate the original flow matching loss equation (details provided in A.2) to explicitly account for the discrepancies between the non-Gaussian initial distribution and the target distribution. Let $\mathbf{x}_t$ denote a linear probability path, starting from a purely noisy initial point $\mathbf{x}_0 \sim \mathcal{N}(0, I)$ and progressing towards a data point $\mathbf{x}_1 \sim \mathcal{D}$. It is defined

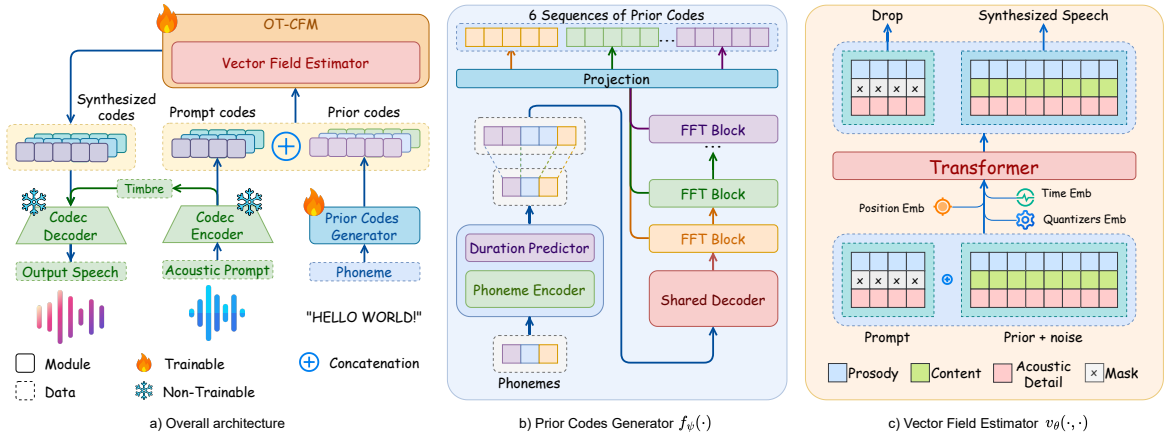

Figure 1: Overview of OZSpeech: (a) The overall architecture: The text prompt is converted to phonemes and then into prior codes via the Prior Codes Generator. Simultaneously, the audio prompt is encoded into codes using the FACodec Encoder. These codes are concatenated along the sequence dimension and fed into the OT-CFM Vector Field Estimator, which generates codes preserving the text content and acoustic attributes. Finally, the FACodec Decoder converts them into output speech. (b) The Prior Codes Generator $f_\psi(\cdot)$ produces sequences of phoneme-aligned codes. (c) The Vector Field Estimator refines these codes with the prosody and acoustic details from the acoustic prompt. Before being fed through $v_\theta(\cdot,\cdot)$, six sequences of codes are first enhanced via Quantizer Embedding, which serves as an identifier for each sequence within the hidden space. These embeddings are then folded along the hidden dimension and processed by the network to estimate the velocity of the prior codes.

as $\mathbf{x}_t = t\mathbf{x}_1 + (1-t)\mathbf{x}_0$, where $t \sim \mathcal{U}(0,1)$ denotes the interpolation parameter. Based on this, the initial point $\mathbf{x}_0$ can be derived as $\mathbf{x}_0 = \frac{t\mathbf{x}_1 - \mathbf{x}_t}{1-t}$. Thus, the OT-CFM objective, as presented in Eq. (12), can be reformulated as follows:

$$\mathcal{L}_{CFM}(\theta) = \mathbb{E}_{t,\mathbf{x}_0,\mathbf{x}_1} \left\| \mathbf{v}_\theta(\mathbf{x}_t, t) - \frac{\mathbf{x}_1 - \mathbf{x}_t}{1-t} \right\|^2. \tag{2}$$

We assume that $\mathbf{x}_t$ can be estimated via $\mathbf{f}_\psi(\cdot)$. Under this assumption, $\mathbf{x}_t$ is treated as a learnable state, which we denote as $\mathbf{x}_{\text{pr}}$, while t is regarded as an unknown interpolation parameter, represented as a prior-dependent time variable τ. Consequently, Eq. (2) can be reformulated as follows:

$$\mathcal{L}_{\text{CFM}}(\theta) = \mathbb{E}_{\mathbf{x}_{\text{pr}},\mathbf{x}_1} \left\| \mathbf{v}_\theta(\mathbf{x}_{\text{pr}}, \tau) - \frac{\mathbf{x}_1 - \mathbf{x}_{\text{pr}}}{1-\tau} \right\|^2. \tag{3}$$

This paradigm is similar to the original OT-CFM in its objective of regressing the velocity between the initial prior $\mathbf{x}_0$ and data $\mathbf{x}_1$ pairs. However, unlike the original approach, it does not access the distribution of $\mathbf{x}_0$ during training. Therefore, it also does not enforce $\mathbf{x}_0$ to follow a normal distribution. Furthermore, as the prior distribution $\mathbf{x}_{\text{pr}}$ approaches the target distribution $\mathbf{x}_1$, both the number of sampling steps and the magnitude of each step are substantially reduced. This convergence enables the sampling process to be efficiently performed in as few as a single step.

Vector Field Estimator Modeling. To model $\mathbf{v}_\theta(\cdot,\cdot)$, we define the latent representations of the prior, target, and estimated target distributions as $\mathbf{x}_{\text{pr}}$, $\mathbf{x}_1$, and $\tilde{\mathbf{x}}_1$, respectively, where $\mathbf{x}_{\text{pr}}, \mathbf{x}_1, \tilde{\mathbf{x}}_1 \in \mathbb{R}^{6\times N\times D}$. These terms represent six quantizer categories with sequence length N and feature dimensionality D. Inspired by diffusion-based text generation models like Diffuseq (Gong et al., 2023), Difformer (Gao et al., 2024), and FlowSeq (Hu et al., 2024), we condition $\mathbf{x}_{\text{pr}}$ on an acoustic prompt to guide $\mathbf{v}_\theta(\cdot,\cdot)$ in transferring speech attributes other than content. Specifically, only prosody and acoustic detail codes serve as prompts, while the content codes are masked to prevent undesired content transfer. The input to $\mathbf{v}_\theta(\cdot,\cdot)$ is then formulated as the concatenated representation:

$$\mathbf{z}_{\text{pr}} = \textbf{Concat}(\mathbf{y}_{\text{mask}}, \mathbf{x}_{\text{pr}} + \epsilon), \quad \epsilon \sim \mathcal{N}(0, I),$$

where $\mathbf{z}_{\text{pr}} \in \mathbb{R}^{6\times L\times D}$, with $L = M + N$ representing the total sequence length of the concatenated input. $\mathbf{y}_{\text{mask}}$ denotes the content-masking representation of the acoustic prompt. Random Gaussian noise ϵ is added to the latent representation of $\mathbf{x}_{\text{pr}}$ to ensure the robustness and diversity of the model. The diagram of the Vector Field Estimator is shown in Fig. 1c.

Folding Mechanism and Quantizer Encoding. Our data representation consists of six sequences of quantizer embeddings, making direct sequence modeling with Transformers challenging. Previ-

ous works using Neural Codec for audio discretization, such as VALL-E (Chen et al., 2025), VALL-E 2 (Chen et al., 2024a), and *NaturalSpeech3* (Ju et al., 2024b), model each quantizer sequence independently. While effective, this approach incurs high computational costs and long generation times due to sequential processing. To mitigate these inefficiencies, we propose modeling all six quantizers simultaneously by folding them along the hidden dimension. Let $\mathcal{F}(\cdot)$ be the folding function, defined as a composition of two transformations: $\mathcal{G} : \mathbb{R}^{6\times L\times D} \rightarrow \mathbb{R}^{L\times 6D}$ and $\mathcal{H} : \mathbb{R}^{L\times 6D} \rightarrow \mathbb{R}^{6D\times D'}$. Thus, $\mathcal{F}$ is expressed as: $\mathcal{F} \triangleq \mathcal{H} \circ \mathcal{G} : \mathbb{R}^{6\times L\times D} \rightarrow \mathbb{R}^{6D\times D'}$. Within this framework, the function $\mathcal{F}(\cdot)$ permutes and reshapes the input tensor to sequentially align the component quantizers in the hidden space, following the prescribed order of prosody, content, and acoustic details. Subsequently, it adjusts the tensor's dimensionality accordingly. In addition, we propose a quantizer encoding mechanism designed to identify specific quantizers within the hidden space. This mechanism operates in conjunction with the $\mathcal{F}(\cdot)$ function. The quantizer encoding is formally defined as follows:

$$\mathcal{Q}(x) = x + \mathbf{Dup}(\omega, L), \quad x \in \mathbb{R}^{6\times L\times D}.$$

Here, the quantizer encoding function $\mathcal{Q}(\cdot)$ integrates the input tensor $\mathbb{R}^{6\times L\times D}$ with the embedding $\mathbf{Dup}(\omega, L)$. In this context, $\omega \in \mathbb{R}^{6\times 1\times D}$ plays a role as the identifier for the latent representation of the quantizers, while the function $\mathbf{Dup}(\cdot,\cdot)$ duplicates the identifier along the sequence length L. With $\mathcal{Q}(\cdot)$, we aim to prevent the model from confusing the quantizers with each other, even when they are simultaneously modeled within a single sequence. Consequently, the latent representation $\mathbf{z}_{\text{pr}}$ is transformed into $\breve{\mathbf{z}}_{\text{pr}}$, which subsequently serves as the direct input to the function $\mathbf{v}_\theta(\cdot,\cdot)$. The transformation is defined as $\breve{\mathbf{z}}_{\text{pr}} = (\mathcal{F} \circ \mathcal{Q})(\mathbf{z}_{\text{pr}})$.

Anchor Loss. To optimize generative model performance on discrete token data and stabilize training, we use Anchor Loss $\mathcal{L}_{anchor}$ as a regularization term for embeddings. Initially introduced in diffusion models for discrete data (Gao et al., 2024) and later adapted for flow matching models (Hu et al., 2024), $\mathcal{L}_{anchor}$ measures the difference between an intermediate state $\mathbf{x}_t$ and the ground truth $\mathbf{x}_1$. It prevents embedding collapse, reduces distances between states, and enables efficient sampling. In this study, $\mathcal{L}_{\text{anchor}}$ minimizes the negative log-likelihood of the joint probability (Eq. (4)).

Let $\mathbf{e}_\phi(\cdot) = [e_1, e_2, \ldots, e_V] \in \mathbb{R}^{V\times D}$ denotes the embedding lookup function with the vocabulary size of V. Given $\mathcal{A}^{6\times L} = \{\alpha_{i,j} \mid i = 1\ldots 6; j = 1\ldots L\}$, where $\alpha_{i,j} \in \{1\ldots V\}$, represents a quantizer element of an $\mathbf{x}_1$ with the sequence length of L, the embedding of $\mathcal{A}^{6\times L}$ can be expressed as $\mathbf{e}_\phi(\mathcal{A}^{6\times L}) = \{\varepsilon_{i,j} \mid i = 1\ldots 6; j = 1\ldots L\}$, where $\varepsilon_{i,j} \in \mathbb{R}^D$. Thus, the joint probability approximating the target distribution $\mathbf{z}_1$, conditioned on the estimated sequences $\tilde{\mathbf{z}}_1$, can be expressed as follows:

$$p(\mathbf{z}_1 \mid \tilde{\mathbf{z}}_1; \phi) = \prod_{i=1}^{6}\prod_{j=1}^{L} p(\varepsilon_{i,j} \mid \tilde{\varepsilon}_{i,j}; \mathbf{e}_\phi), \quad (4)$$

where $\tilde{\mathbf{z}}_1$ is the approximation of $\mathbf{z}_1$, deduced using the triplet consisting of the estimated vector $\mathbf{v}_\theta(\breve{\mathbf{z}}_{\text{pr}}, \tau)$, the prior state $\mathbf{z}_{\text{pr}}$, and the corresponding interpolate parameter τ. The function $\mathcal{F}^{-1}$ denotes the reverse function of $\mathcal{F}$. This relationship is expressed as $\tilde{\mathbf{z}}_1 = \mathbf{z}_{\text{pr}} + (1-\tau)\mathcal{F}^{-1}(\mathbf{v}_\theta(\breve{\mathbf{z}}_{\text{pr}}, \tau))$.

Total loss. We define the total loss function used in our joint training method as $\mathcal{L}_{total} = \mathcal{L}_{prior} + \mathcal{L}_{dur} + \mathcal{L}_{CFM} + \mathcal{L}_{anchor}$. The loss functions $\mathcal{L}_{prior}$ and $\mathcal{L}_{dur}$ set the training objective for the Prior Codes Generator, whereas $\mathcal{L}_{CFM}$ and $\mathcal{L}_{anchor}$ are designed to construct the vector field and distill the sampling steps, respectively.

4 Experiments

4.1 Experiment Setup

Dataset. We employ the *LibriTTS* dataset (Zen et al., 2019), which comprises multi-speaker English audio recordings of training data. For benchmarking purposes, we use the *LibriSpeech test-clean* (Panayotov et al., 2015) dataset. More detailed information is provided in Appendix D.1.

Evaluation Metrics. To assess model performance, we employ the following objective evaluation metrics for each criterion: speech quality, quantified by UTMOS; speaker similarity, measured using SIM-O and SIM-R; robustness, indicated by WER; and prosody accuracy and error, analyzed through pitch and energy. Additionally, we employ NFE and RTF metrics to measure the latency of the sampling process. More details on the evaluation metrics can be found in Appendix D.2.

Table 1: Performance evaluation on the *LibriSpeech test-clean* across different audio prompt lengths. **Bold** indicates the best result, and underline indicates the second-best result. (↑) indicates that higher values are better, while (↓) indicates that lower values are better. [♠] means reproduced results. [★] and [♣] mean results inferred from official and ufficial checkpoints, respectively. Abbreviation: LT (LibriTTS), E (Emilia), GS (GigaSpeech).

				SPK-SIM		F0		Energy	
Model	**Data (hours)**	**UTMOS (↑)**	**WER (↓)**	**SIM-O (↑)**	**SIM-R (↑)**	**Accuracy (↑)**	**RMSE (↓)**	**Accuracy (↑)**	**RMSE (↓)**
Ground Truth		4.09	0.02	-	-	-	-	-	-
1s Prompt									
F5-TTS [★] (Chen et al., 2024c)	E (95,000)	1.35	0.20	0.11	-	0.51	43.65	0.36	0.42
VoiceCraft [★] (Peng et al., 2024)	GS (9,000)	3.45	0.16	**0.31**	0.24	0.61	31.57	**0.52**	**0.01**
NaturalSpeech 2 [♣] (Shen et al., 2024)	LT (585)	2.12	0.12	0.20	0.21	**0.69**	**26.48**	0.39	0.02
VALL-E [♠] (Chen et al., 2025)	LT (500)	**3.61**	0.21	0.24	0.28	0.55	37.87	0.40	0.02
OZSpeech	LT (500)	3.17	**0.05**	0.30	**0.33**	0.62	27.7	0.49	0.02
3s Prompt									
F5-TTS [★] (Chen et al., 2024c)	E (95,000)	1.25	0.30	0.18	-	0.40	64.06	0.44	0.43
VoiceCraft [★] (Peng et al., 2024)	GS (9,000)	3.55	0.18	**0.51**	0.45	0.78	17.22	0.44	**0.01**
NaturalSpeech 2 [♣] (Shen et al., 2024)	LT (585)	2.38	0.09	0.31	0.38	0.80	15.62	0.25	0.02
VALL-E [♠] (Chen et al., 2025)	LT (500)	**3.68**	0.19	0.40	**0.48**	0.75	21.66	0.36	0.02
OZSpeech	LT (500)	3.15	**0.05**	0.40	0.47	**0.81**	**11.96**	**0.67**	**0.01**
5s Prompt									
F5-TTS [★] (Chen et al., 2024c)	E (95,000)	1.24	0.34	0.21	-	0.33	66.97	0.40	0.44
VoiceCraft [★] (Peng et al., 2024)	GS (9,000)	3.58	0.19	**0.56**	0.51	0.81	14.48	0.46	**0.01**
NaturalSpeech 2 [♣] (Shen et al., 2024)	LT (585)	2.33	0.09	0.35	0.44	0.84	13.13	0.28	0.02
VALL-E [♠] (Chen et al., 2025)	LT (500)	**3.72**	0.19	0.46	**0.55**	0.79	18.20	0.41	**0.01**
OZSpeech	LT (500)	3.15	**0.05**	0.39	0.48	0.83	**12.05**	**0.67**	**0.01**

Baselines. We compare our model with previous zero-shot TTS baselines. Further details regarding baselines are available in Appendix D.3.

4.2 Main Results

Table 1 shows the performance of OZSpeech and representative baseline methods for 1s, 3s, and 5s audio prompt lengths. OZSpeech establishes a new SOTA on WER across all audio prompt lengths, demonstrating superior content preserving capability through a *multi-fold* reduction in WER. For example, OZSpeech reduces WER by a factor of $1.8 - 6.8$ over the other methods for 5s prompt length. Some of these models, such as F5-TTS, are trained on substantially more training data (F5-TTS is trained on 95,000 hours of speech whereas OZSpeech is trained on 500 hours). Compared to the next-best method, OZSpeech yields a relative reduction in WER by 58%, 44%, and 44% for 1s, 3s, and 5s audio prompt lengths, respectively. Additionally, while the WER scores of all baseline methods are sensitive to prompt length, OZSpeech maintains a consistent WER regardless of prompt length.

For pitch and energy accuracies and errors, which indicate the prosody reconstruction ability of TTS systems, OZSpeech consistently ranks as the best or second-best performer across different prompt lengths. For the remaining metrics (UTMOS, SIM-O, and SIM-R), our method in overall does not exhibit an obvious performance advantage over the baseline models. (We note that these models also experience trade-offs between different metrics.) However, our goal is to enhance the balance between intelligibility (i.e. content accuracy) and acoustical/perceptual quality while maintaining low latency and small model size.

Our UTMOS scores show a rather small degradation compared to some of the baselines, particularly VALL-E and VoiceCraft. This is largely due to differences in the neural codecs' trade-offs between acoustic and semantic representations. EnCodec (VoiceCraft's codec) primarily relies on acoustic codes, while SpeechTokenizer (VALL-E's codec in this experiment) incorporates one semantic sequence alongside acoustic codes. In contrast, FaCodec (OZSpeech's codec) strives to balance both representations. However, our focus is on optimizing the trade-off between sampling speed and speech synthesis quality.

We also retrain F5-TTS with 500 hours of the LibriTTS dataset using the official code for 1 million steps following its guideline, however the resulting WER exceeds 0.95 across all settings, so we exclude this retrained checkpoint from Table 1 and instead use the officially released checkpoint, which is trained on 95,000 hours of data. The poor retraining results suggest that this method, which is based on traditional OT-CFM, requires a much larger, more diverse dataset for robustness. In contrast, neural codec-based models remain effective with limited data, likely due to extensive pre-training of the neural codec module on massive datasets. Thus, traditional OT-CFM methods like

Table 2: Comparison of model size and latency for 3s audio prompt length. Column **#Params** indicates the total number of parameters required for end-to-end synthesis, with the first value representing the parameters of the zero-shot model (trainable) and the second value corresponding to those of the neural codec or vocoder component (frozen).

Model	#Params	NFE (↓)	RTF (↓)	WER (↓)	SIM-O (↑)
F5-TTS (Eskimez et al., 2024)	336M + 13.5M Vovos (Siuzdak, 2024)	32	0.70	0.30	0.18
VoiceCraft (Peng et al., 2024)	830M + 14M EnCodec (Défossez et al., 2023)	-	1.70	0.18	**0.51**
NaturalSpeech 2 (Shen et al., 2024)	378M + 14M EnCodec (Défossez et al., 2023)	200	1.66	0.09	0.31
VALL-E (Chen et al., 2025)	594M + 104M SpeechTokenizer (Zhang et al., 2024a)	-	0.86	0.19	0.40
OZSpeech	145M + 102M FACodec (Ju et al., 2024b)	**1**	**0.26**	**0.05**	0.40

Table 3: Comparison of two prompting strategies during training: *First Segment* and *Arbitrary Segment*.

Prompt Setting	UTMOS (↑)	WER (↓)	SPK-SIM	
			SIM-O (↑)	SIM-R (↑)
1s Prompt				
First segment	3.01	0.08	0.25	0.29
Arbitrary segment	**3.17**	**0.05**	**0.30**	**0.33**
3s Prompt				
First segment	3.04	0.08	0.35	0.42
Arbitrary segment	**3.15**	**0.05**	**0.40**	**0.47**
5s Prompt				
First segment	3.02	0.06	0.37	0.45
Arbitrary segment	**3.15**	**0.05**	**0.39**	**0.48**

F5-TTS are unsuitable for low-resource languages.

Table 2 compares the model sizes and latency of OZSpeech and baseline models. OZSpeech is the smallest model of all, being only 29%-71% the size of the other models. When considering only the trainable part of the models, the number of trainable parameters of OZSpeech is only 17%-43% that of the other models. For the NFE metric, our model uses only a single sampling step, significantly reducing computation compared to NaturalSpeech 2 and F5-TTS, which require 200 and 32 steps, respectively, to achieve optimal performance. As a result, in terms of inference speed represented by the RTF metric, OZSpeech is almost 3 times faster than the next fastest model, F5-TTS.

4.3 Ablation Study

Table 3 compares the performance of two prompting strategies: *First Segment* and *Arbitrary Segment*. The former generates prompts using the initial portion of the ground truth, whereas the latter selects random audio segments from the ground truth to form the prompts. The results clearly show that the *Arbitrary Segment* strategy outperforms the *First Segment* strategy across all metrics. In the *First Segment* setting, the model seems to overfit in that it is forced to transfer the prompt to the beginning of the target. In contrast, the *Arbitrary Segment* setting hides the position of the prompt, allowing it to smoothly transfer attributes from the prompt to the target. Consequently, we adopt the *Arbitrary Segment* approach for our training. This experiment also shows that the *Arbitrary Segment* approach improves robustness by exposing the model to a more diverse range of speech contexts, leading to better generalization in zero-shot speech synthesis.

4.4 Noise Tolerance Analysis

Unlike previous studies, we propose to investigate the effects of noisy prompts in TTS. Table 4 evaluates the tolerance of each model on noisy prompts. We conduct *zero-shot* testing of all models in this scenario, where zero-shot in this context means that the models trained on their original training dataset, typically with clean prompts, are directly tested on noisy prompts. For this, we generate three sets of noisy prompts at SNRs of 0dB, 6dB, and 12dB, respectively. SNR $= \infty$ refers to prompts directly sourced from *LibriSpeech test-clean* dataset, with metric values directly replicated from Table 1.

Overall, all baseline methods are highly sensitive to noise in the audio prompts, experiencing significant degradation in all metrics as prompt SNR decreases. OZSpeech also shows similar sensitivity except for WER, which experiences either no or negligible degradation across all prompt SNR levels. VALL-E seems to be the most vulnerable to noise, where the WER increases by almost 2.7 times at the least noisy setting, SNR = 12dB. At SNR = 0dB, VALL-E becomes almost unintelligible with a 93% WER. The WER results highlight the robust intelligibility of OZSpeech, even in noisy prompt conditions.

Although OZSpeech performs sub-optimally in non-WER metrics with the original clean prompts, it surpasses all baseline models in UTMOS. This improvement is largely attributed to the significant performance drop observed in the baseline models. Mixed results are observed when comparing all models on the remaining metrics.

Next, we further fine-tune OZSpeech with both

Table 4: Performance evaluation on noisy audio prompts. The noisy prompts are derived from the *LibriSpeech test-clean* dataset with additive noise augmentation. The prompts are 3-second long. The checkpoints of each model trained on *LibriTTS*—except for VoiceCraft, which was trained on *GigaSpeech*—are used without re-training the models to include noisy samples. [⧫] means fine-tuned results on noisy prompts. This table highlights a vulnerable use case where speech prompts contain noise, assessing the tolerance of these models. SNR= ∞ indicates the prompts are directly obtained from *LibriSpeech test-clean* dataset and these results are simply copied from Table 1.

				SPK-SIM		F0		Energy	
SNR (dB)	**Model**	**UTMOS** (↑)	**WER** (↓)	**SIM-O** (↑)	**SIM-R** (↑)	**Accuracy** (↑)	**RMSE** (↓)	**Accuracy** (↑)	**RMSE** (↓)
∞	F5-TTS (Chen et al., 2024c)	1.25	0.30	0.18	-	0.40	64.06	0.44	0.43
	VoiceCraft (Peng et al., 2024)	3.55	0.18	**0.51**	0.45	0.78	17.22	0.44	**0.01**
	NaturalSpeech 2 (Shen et al., 2024)	2.38	0.09	0.31	0.38	0.80	15.62	0.25	0.02
	VALL-E (Chen et al., 2025)	**3.68**	0.19	0.40	**0.48**	0.75	21.66	0.36	0.02
	OZSpeech	3.15	**0.05**	0.39	0.47	**0.81**	**11.96**	**0.67**	**0.01**
	OZSpeech [⧫]	3.19	0.06	0.39	0.46	0.78	13.67	0.65	**0.01**
12	F5-TTS (Chen et al., 2024c)	1.34	0.22	0.10	-	0.36	52.79	0.44	0.42
	VoiceCraft (Peng et al., 2024)	2.42	0.20	**0.40**	**0.40**	0.59	32.48	0.60	**0.01**
	NaturalSpeech 2 (Shen et al., 2024)	1.66	0.12	0.22	0.34	0.71	20.0	0.45	**0.01**
	VALL-E (Chen et al., 2025)	2.43	0.51	0.25	0.31	0.54	59.25	0.40	0.02
	OZSpeech	2.65	**0.05**	0.28	0.35	0.70	21.70	0.53	0.03
	OZSpeech [⧫]	**3.04**	**0.05**	0.33	0.39	**0.76**	**15.0**	**0.73**	**0.01**
6	F5-TTS (Chen et al., 2024c)	1.41	0.31	0.06	-	0.35	60.47	0.44	0.35
	VoiceCraft (Peng et al., 2024)	1.80	0.27	**0.33**	**0.36**	0.50	45.31	0.68	**0.01**
	NaturalSpeech 2 (Shen et al., 2024)	1.42	0.16	0.17	0.30	0.61	27.41	0.58	**0.01**
	VALL-E (Chen et al., 2025)	1.66	0.77	0.14	0.18	0.40	96.93	0.44	0.02
	OZSpeech	2.21	**0.06**	0.23	0.29	0.61	32.80	0.46	0.05
	OZSpeech [⧫]	**2.90**	**0.06**	0.29	0.34	**0.72**	**17.41**	**0.74**	**0.01**
0	F5-TTS (Chen et al., 2024c)	1.43	0.49	0.05	-	0.35	64.29	0.44	0.22
	VoiceCraft (Peng et al., 2024)	1.58	0.44	0.22	**0.29**	0.40	57.40	0.55	0.02
	NaturalSpeech 2 (Shen et al., 2024)	1.33	0.23	0.12	0.26	0.48	38.27	**0.56**	**0.01**
	VALL-E (Chen et al., 2025)	1.44	0.93	0.07	0.11	0.36	102,68	0.52	0.07
	OZSpeech	1.72	**0.06**	0.17	0.22	0.45	46.60	0.44	0.08
	OZSpeech [⧫]	**2.58**	**0.06**	**0.23**	0.28	**0.67**	**21.37**	0.54	0.02

original and noisy prompts, where noisy prompts occur with a probability of 0.8. The noisy prompts are constructed by mixing the original prompts with random noise at different SNRs, drawn from a uniform distribution over the [0dB, 15dB] range. We leveraged the QUT-NOISE database (Dean et al., 2010) as our noise dataset. When tested with clean prompts (SNR = ∞), there is either no change or minimal changes in OZSpeech's performance across all metrics before and after fine-tuning. In noisy prompt conditions, WER remains unaffected by fine-tuning while the other metrics are significantly improved across all SNR levels. With decreasing SNR, fine-tuning generally yields increasingly larger improvements in all non-WER metrics.

We have empirically demonstrated the feasibility of the noise-aware training approach, which aims to synthesize noise-free speech conditioned by noisy prompts. This approach enables Zero-Shot TTS models to implicitly remove noise from given codec codes while preserving key attributes of speech. Consequently, neural codec-based Zero-shot TTS systems, which have traditionally been vulnerable and sensitive to noisy prompts, exhibit enhanced robustness, particularly against adversarial attacks.

5 Conclusion

We propose OZSpeech, an effective and efficient zero-shot TTS model that employs flow matching with a single sampling step from a learned prior instead of random noise. The model strikes a balance between synthesized speech intelligibility and acoustical quality. In particular, OZSpeech yields a multi-fold improvement in WER compared to existing baseline methods with some trade-off in the auditory quality. Furthermore, unlike other methods, OZSpeech achieves a consistent WER across different audio prompt's lengths and noise levels. With a single-step sampling approach and a novel prior learning module that learns an effective starting point for the sampling process, our model requires significantly less computation, with inference speed being $2.7 - 6.5$ times faster than the other methods. In addition, our model size is only 29%-71% that of the other models. OZSpeech achieves competitive results even over models that are trained on much larger training sets.

In future work, we plan to enhance OZSpeech by integrating adaptive noise filtering techniques and expanding its capability to support multilingual and multimodal zero-shot speech synthesis, enabling more versatile applications in real-world scenarios.

Limitations

Despite achieving remarkable results, our Zero-shot TTS model still encounters challenges in naturalness. We have observed that the synthesized speech often exhibits slight distortions, which appear to contribute to a degradation in overall quality. In this study, we employed the Duration Predictor, originally proposed in FastSpeech (Ren et al., 2019b), to align input phonemes with codec codes. This module requires ground-truth phoneme durations for training; however, since phoneme durations are inherently real numbers rather than integers, inaccuracies arise in the ground-truth data. To align with codec codes, these durations must be rounded to integer values, which subsequently degrades the quality of the synthesized speech in the temporal domain. To address this issue in future work, we plan to explore alternative alignment methods, such as Monotonic Alignment Search (Kim et al., 2020) or Encoder-Decoder architectures. Nevertheless, the approach employed in this study remains the de facto approach in many real-world TTS systems, where latency is a critical factor. Thus, this presents a trade-off between synthesis quality and computational efficiency.

Potential Risks

Zero-shot Text-to-Speech (TTS) models offer several advantages, such as the ability to rapidly and effortlessly synthesize speech without requiring repeated recordings, making them particularly beneficial for content creators and for restoring damaged audio. However, despite these benefits, they also pose significant risks. Zero-shot TTS models, which can generate speech in novel voices with little to no training data, present several potential threats, including:

- **Deepfake Fraud:** Malicious entities may exploit these models to impersonate individuals, facilitating scams, misinformation, or fraudulent activities.
- **Fabricated Media:** Synthesized audio can be used to create misleading or defamatory content, influencing public perception and spreading misinformation.
- **Privacy Violations:** The unauthorized replication of voices without explicit consent raises ethical and legal concerns regarding individual privacy.
- **Legal and Copyright Challenges:** Certain voices may be subject to copyright, trademark, or publicity rights protections, potentially leading to legal disputes over their unauthorized use.

References

Guoguo Chen, Shuzhou Chai, Guan-Bo Wang, Jiayu Du, Wei-Qiang Zhang, Chao Weng, Dan Su, Daniel Povey, Jan Trmal, Junbo Zhang, Mingjie Jin, Sanjeev Khudanpur, Shinji Watanabe, Shuaijiang Zhao, Wei Zou, Xiangang Li, Xuchen Yao, Yongqing Wang, Zhao You, and Zhiyong Yan. 2021. Gigaspeech: An evolving, multi-domain asr corpus with 10,000 hours of transcribed audio. In *Interspeech 2021*, pages 3670–3674.

Sanyuan Chen, Shujie Liu, Long Zhou, Yanqing Liu, Xu Tan, Jinyu Li, Sheng Zhao, Yao Qian, and Furu Wei. 2024a. Vall-e 2: Neural codec language models are human parity zero-shot text to speech synthesizers. *Preprint*, arXiv:2406.05370.

Sanyuan Chen, Shujie Liu, Long Zhou, Yanqing Liu, Xu Tan, Jinyu Li, Sheng Zhao, Yao Qian, and Furu Wei. 2024b. Vall-e 2: Neural codec language models are human parity zero-shot text to speech synthesizers. *arXiv preprint arXiv:2406.05370*.

Sanyuan Chen, Chengyi Wang, Yu Wu, Ziqiang Zhang, Long Zhou, Shujie Liu, Zhuo Chen, Yanqing Liu, Huaming Wang, Jinyu Li, Lei He, Sheng Zhao, and Furu Wei. 2025. Neural codec language models are zero-shot text to speech synthesizers. *IEEE Transactions on Audio, Speech and Language Processing*, pages 1–15.

Yushen Chen, Zhikang Niu, Ziyang Ma, Keqi Deng, Chunhui Wang, Jian Zhao, Kai Yu, and Xie Chen. 2024c. F5-tts: A fairytaler that fakes fluent and faithful speech with flow matching. *Preprint*, arXiv:2410.06885.

David Dean, Sridha Sridharan, Robert Vogt, and Michael Mason. 2010. The qut-noise-timit corpus for evaluation of voice activity detection algorithms. In *Proceedings of the 11th annual conference of the international speech communication association*, pages 3110–3113. International Speech Communication Association.

Alexandre Défossez, Jade Copet, Gabriel Synnaeve, and Yossi Adi. 2023. High fidelity neural audio compression. *Transactions on Machine Learning Research*. Featured Certification, Reproducibility Certification.

Chenpeng Du, Yiwei Guo, Feiyu Shen, Zhijun Liu, Zheng Liang, Xie Chen, Shuai Wang, Hui Zhang, and Kai Yu. 2024a. Unicats: A unified context-aware text-to-speech framework with contextual vq-diffusion and vocoding. *Proceedings of the AAAI Conference on Artificial Intelligence*, 38(16):17924–17932.

Zhihao Du, Qian Chen, Shiliang Zhang, Kai Hu, Heng Lu, Yexin Yang, Hangrui Hu, Siqi Zheng, Yue

Gu, Ziyang Ma, et al. 2024b. Cosyvoice: A scalable multilingual zero-shot text-to-speech synthesizer based on supervised semantic tokens. *arXiv preprint arXiv:2407.05407*.

Sefik Emre Eskimez, Xiaofei Wang, Manthan Thakker, Canrun Li, Chung-Hsien Tsai, Zhen Xiao, Hemin Yang, Zirun Zhu, Min Tang, Xu Tan, Yanqing Liu, Sheng Zhao, and Naoyuki Kanda. 2024. E2 TTS: Embarrassingly easy fully non-autoregressive zero-shot TTS. *Preprint*, arXiv:2406.18009.

Kevin Frans, Danijar Hafner, Sergey Levine, and Pieter Abbeel. 2024. One step diffusion via shortcut models. *Preprint*, arXiv:2410.12557.

Zhujin Gao, Junliang Guo, Xu Tan, Yongxin Zhu, Fang Zhang, Jiang Bian, and Linli Xu. 2024. Empowering diffusion models on the embedding space for text generation. In *Proceedings of the 2024 Conference of the North American Chapter of the Association for Computational Linguistics: Human Language Technologies (Volume 1: Long Papers)*, pages 4664–4683, Mexico City, Mexico. Association for Computational Linguistics.

Shansan Gong, Mukai Li, Jiangtao Feng, Zhiyong Wu, and Lingpeng Kong. 2023. Diffuseq: Sequence to sequence text generation with diffusion models. In *The Eleventh International Conference on Learning Representations*.

Anmol Gulati, James Qin, Chung-Cheng Chiu, Niki Parmar, Yu Zhang, Jiahui Yu, Wei Han, Shibo Wang, Zhengdong Zhang, Yonghui Wu, and Ruoming Pang. 2020. Conformer: Convolution-augmented transformer for speech recognition. In *Interspeech 2020*, pages 5036–5040.

Zhifang Guo, Yichong Leng, Yihan Wu, Sheng Zhao, and Xu Tan. 2022. Prompttts: Controllable text-to-speech with text descriptions. *Preprint*, arXiv:2211.12171.

Bing Han, Long Zhou, Shujie Liu, Sanyuan Chen, Lingwei Meng, Yanming Qian, Yanqing Liu, Sheng Zhao, Jinyu Li, and Furu Wei. 2024. Vall-e r: Robust and efficient zero-shot text-to-speech synthesis via monotonic alignment. *arXiv preprint arXiv:2406.07855*.

Haorui He, Zengqiang Shang, Chaoren Wang, Xuyuan Li, Yicheng Gu, Hua Hua, Liwei Liu, Chen Yang, Jiaqi Li, Peiyang Shi, Yuancheng Wang, Kai Chen, Pengyuan Zhang, and Zhizheng Wu. 2024. Emilia: An extensive, multilingual, and diverse speech dataset for large-scale speech generation. In *Proc. of SLT*.

Jonathan Ho, Ajay Jain, and Pieter Abbeel. 2020. Denoising diffusion probabilistic models. In *Advances in Neural Information Processing Systems*, volume 33, pages 6840–6851. Curran Associates, Inc.

Vincent Hu, Di Wu, Yuki Asano, Pascal Mettes, Basura Fernando, Björn Ommer, and Cees Snoek. 2024. Flow matching for conditional text generation in a few sampling steps. In *Proceedings of the 18th Conference of the European Chapter of the Association for Computational Linguistics (Volume 2: Short Papers)*, pages 380–392, St. Julian's, Malta. Association for Computational Linguistics.

Shengpeng Ji, Ziyue Jiang, Hanting Wang, Jialong Zuo, and Zhou Zhao. 2024a. MobileSpeech: A fast and high-fidelity framework for mobile zero-shot text-to-speech. In *Proceedings of the 62nd Annual Meeting of the Association for Computational Linguistics (Volume 1: Long Papers)*, pages 13588–13600, Bangkok, Thailand. Association for Computational Linguistics.

Shengpeng Ji, Jialong Zuo, Minghui Fang, Ziyue Jiang, Feiyang Chen, Xinyu Duan, Baoxing Huai, and Zhou Zhao. 2024b. Textrolspeech: A text style control speech corpus with codec language text-to-speech models. In *ICASSP 2024 - 2024 IEEE International Conference on Acoustics, Speech and Signal Processing (ICASSP)*, pages 10301–10305.

Zeqian Ju, Yuancheng Wang, Kai Shen, Xu Tan, Detai Xin, Dongchao Yang, Eric Liu, Yichong Leng, Kaitao Song, Siliang Tang, Zhizheng Wu, Tao Qin, Xiangyang Li, Wei Ye, Shikun Zhang, Jiang Bian, Lei He, Jinyu Li, and sheng zhao. 2024a. Naturalspeech 3: Zero-shot speech synthesis with factorized codec and diffusion models. In *Forty-first International Conference on Machine Learning*.

Zeqian Ju, Yuancheng Wang, Kai Shen, Xu Tan, Detai Xin, Dongchao Yang, Eric Liu, Yichong Leng, Kaitao Song, Siliang Tang, Zhizheng Wu, Tao Qin, Xiangyang Li, Wei Ye, Shikun Zhang, Jiang Bian, Lei He, Jinyu Li, and Sheng Zhao. 2024b. NaturalSpeech 3: Zero-shot speech synthesis with factorized codec and diffusion models. In *Proceedings of the 41st International Conference on Machine Learning*, volume 235 of *Proceedings of Machine Learning Research*, pages 22605–22623. PMLR.

Minki Kang, Wooseok Han, Sung Ju Hwang, and Eunho Yang. 2023. Zet-speech: Zero-shot adaptive emotion-controllable text-to-speech synthesis with diffusion and style-based models. In *Interspeech 2023*, pages 4339–4343.

Eugene Kharitonov, Damien Vincent, Zalán Borsos, Raphaël Marinier, Sertan Girgin, Olivier Pietquin, Matt Sharifi, Marco Tagliasacchi, and Neil Zeghidour. 2023. Speak, read and prompt: High-fidelity text-to-speech with minimal supervision. *Transactions of the Association for Computational Linguistics*, 11:1703–1718.

Jaehyeon Kim, Sungwon Kim, Jungil Kong, and Sungroh Yoon. 2020. Glow-tts: A generative flow for text-to-speech via monotonic alignment search. *ArXiv*, abs/2005.11129.

Sungwon Kim, Kevin J. Shih, Rohan Badlani, Joao Felipe Santos, Evelina Bakhturina, Mikyas T. Desta, Rafael Valle, Sungroh Yoon, and Bryan Catanzaro.

2023. P-flow: A fast and data-efficient zero-shot TTS through speech prompting. In *Thirty-seventh Conference on Neural Information Processing Systems*.

Matthew Le, Apoorv Vyas, Bowen Shi, Brian Karrer, Leda Sari, Rashel Moritz, Mary Williamson, Vimal Manohar, Yossi Adi, Jay Mahadeokar, and Wei-Ning Hsu. 2023. Voicebox: Text-guided multilingual universal speech generation at scale. In *Thirty-seventh Conference on Neural Information Processing Systems*.

Yaron Lipman, Ricky T. Q. Chen, Heli Ben-Hamu, Maximilian Nickel, and Matthew Le. 2023. Flow matching for generative modeling. In *The Eleventh International Conference on Learning Representations*.

Xingchao Liu, Chengyue Gong, and qiang liu. 2023. Flow straight and fast: Learning to generate and transfer data with rectified flow. In *The Eleventh International Conference on Learning Representations*.

Michael McAuliffe, Michaela Socolof, Sarah Mihuc, Michael Wagner, and Morgan Sonderegger. 2017. Montreal forced aligner: Trainable text-speech alignment using kaldi. In *Interspeech 2017*, pages 498–502.

Shivam Mehta, Ruibo Tu, Jonas Beskow, Éva Székely, and Gustav Eje Henter. 2024. Matcha-tts: A fast tts architecture with conditional flow matching. In *ICASSP 2024 - 2024 IEEE International Conference on Acoustics, Speech and Signal Processing (ICASSP)*, pages 11341–11345.

Lingwei Meng, Long Zhou, Shujie Liu, Sanyuan Chen, Bing Han, Shujie Hu, Yanqing Liu, Jinyu Li, Sheng Zhao, Xixin Wu, Helen Meng, and Furu Wei. 2024. Autoregressive speech synthesis without vector quantization. *CoRR*, abs/2407.08551.

Vassil Panayotov, Guoguo Chen, Daniel Povey, and Sanjeev Khudanpur. 2015. Librispeech: An asr corpus based on public domain audio books. In *2015 IEEE International Conference on Acoustics, Speech and Signal Processing (ICASSP)*, pages 5206–5210.

Puyuan Peng, Po-Yao Huang, Shang-Wen Li, Abdelrahman Mohamed, and David Harwath. 2024. VoiceCraft: Zero-shot speech editing and text-to-speech in the wild. In *Proceedings of the 62nd Annual Meeting of the Association for Computational Linguistics (Volume 1: Long Papers)*, pages 12442–12462, Bangkok, Thailand. Association for Computational Linguistics.

Yi Ren, Yangjun Ruan, Xu Tan, Tao Qin, Sheng Zhao, Zhou Zhao, and Tie-Yan Liu. 2019a. Fastspeech: Fast, robust and controllable text to speech. In *Advances in Neural Information Processing Systems*, volume 32. Curran Associates, Inc.

Yi Ren, Yangjun Ruan, Xu Tan, Tao Qin, Sheng Zhao, Zhou Zhao, and Tie-Yan Liu. 2019b. *FastSpeech: fast, robust and controllable text to speech*. Curran Associates Inc., Red Hook, NY, USA.

Takaaki Saeki, Detai Xin, Wataru Nakata, Tomoki Koriyama, Shinnosuke Takamichi, and Hiroshi Saruwatari. 2022. Utmos: Utokyo-sarulab system for voicemos challenge 2022. *Preprint*, arXiv:2204.02152.

Kai Shen, Zeqian Ju, Xu Tan, Eric Liu, Yichong Leng, Lei He, Tao Qin, sheng zhao, and Jiang Bian. 2024. Naturalspeech 2: Latent diffusion models are natural and zero-shot speech and singing synthesizers. In *The Twelfth International Conference on Learning Representations*.

Hubert Siuzdak. 2024. Vocos: Closing the gap between time-domain and fourier-based neural vocoders for high-quality audio synthesis. *Preprint*, arXiv:2306.00814.

Yakun Song, Zhuo Chen, Xiaofei Wang, Ziyang Ma, and Xie Chen. 2024. Ella-v: Stable neural codec language modeling with alignment-guided sequence reordering. *Preprint*, arXiv:2401.07333.

Yang Song, Prafulla Dhariwal, Mark Chen, and Ilya Sutskever. 2023. Consistency models. In *Proceedings of the 40th International Conference on Machine Learning*, volume 202 of *Proceedings of Machine Learning Research*, pages 32211–32252. PMLR.

Yang Song, Jascha Sohl-Dickstein, Diederik P Kingma, Abhishek Kumar, Stefano Ermon, and Ben Poole. 2021. Score-based generative modeling through stochastic differential equations. In *International Conference on Learning Representations*.

Chung Tran, Chi Mai Luong, and Sakriani Sakti. 2023. Sten-tts: Improving zero-shot cross-lingual transfer for multi-lingual tts with style-enhanced normalization diffusion framework. In *Interspeech 2023*, pages 4464–4468.

Aaron van den Oord, Oriol Vinyals, and Koray Kavukcuoglu. 2017. Neural discrete representation learning. In *Proceedings of the 31st International Conference on Neural Information Processing Systems*, NIPS'17, page 6309–6318, Red Hook, NY, USA. Curran Associates Inc.

Apoorv Vyas, Bowen Shi, Matthew Le, Andros Tjandra, Yi-Chiao Wu, Baishan Guo, Jiemin Zhang, Xinyue Zhang, Robert Adkins, William Ngan, Jeff Wang, Ivan Cruz, Bapi Akula, Akinniyi Akinyemi, Brian Ellis, Rashel Moritz, Yael Yungster, Alice Rakotoarison, Liang Tan, Chris Summers, Carleigh Wood, Joshua Lane, Mary Williamson, and Wei-Ning Hsu. 2023. Audiobox: Unified audio generation with natural language prompts. *Preprint*, arXiv:2312.15821.

Chengyi Wang, Sanyuan Chen, Yu Wu, Ziqiang Zhang, Long Zhou, Shujie Liu, Zhuo Chen, Yanqing Liu, Huaming Wang, Jinyu Li, et al. 2023. Neural codec language models are zero-shot text to speech synthesizers. *arXiv preprint arXiv:2301.02111*.

Neil Zeghidour, Alejandro Luebs, Ahmed Omran, Jan Skoglund, and Marco Tagliasacchi. 2022.

Soundstream: An end-to-end neural audio codec. *IEEE/ACM Transactions on Audio, Speech, and Language Processing*, 30:495–507.

Heiga Zen, Viet Dang, Rob Clark, Yu Zhang, Ron J. Weiss, Ye Jia, Zhifeng Chen, and Yonghui Wu. 2019. Libritts: A corpus derived from librispeech for text-to-speech. In *Interspeech 2019*, pages 1526–1530.

Xin Zhang, Dong Zhang, Shimin Li, Yaqian Zhou, and Xipeng Qiu. 2024a. Speechtokenizer: Unified speech tokenizer for speech language models. In *The Twelfth International Conference on Learning Representations*.

Xueyao Zhang, Liumeng Xue, Yicheng Gu, Yuancheng Wang, Jiaqi Li, Haorui He, Chaoren Wang, Ting Song, Xi Chen, Zihao Fang, Haopeng Chen, Junan Zhang, Tze Ying Tang, Lexiao Zou, Mingxuan Wang, Jun Han, Kai Chen, Haizhou Li, and Zhizheng Wu. 2024b. Amphion: An open-source audio, music and speech generation toolkit. In *IEEE Spoken Language Technology Workshop, SLT 2024*.

Ziqiang Zhang, Long Zhou, Chengyi Wang, Sanyuan Chen, Yu Wu, Shujie Liu, Zhuo Chen, Yanqing Liu, Huaming Wang, Jinyu Li, et al. 2023. Speak foreign languages with your own voice: Cross-lingual neural codec language modeling. *arXiv preprint arXiv:2303.03926*.

A Background

A.1 FACodec

Factorized neural speech codec, named FACodec, (Ju et al., 2024b) was proposed as a codec disentangler and timbre extractor. It separates the original speech waveform into distinct aspects: content, prosody, acoustic details, and timbre. Specifically, the speech input $x \in \mathbb{R}^C$ is processed through a speech encoder, f_{enc}, comprising several convolutional blocks to produce a pre-quantization latent representation:

$$h = f_{enc}(x) \in \mathbb{R}^{T \times D}, \tag{5}$$

where T and D denote the downsampled timeframes and the latent dimension, respectively. Subsequently, three factorized vector quantizers (FVQs) are employed to tokenize h into distinct discrete sequences, capturing detailed representations of speech attributes such as content, prosody, and acoustic details. Let $\mathcal{Q}_p$, $\mathcal{Q}_c$, and $\mathcal{Q}_a$ denote the FVQs for prosody, content, and acoustic details, respectively. Each FVQ comprises a certain number of quantizers, defined $\mathcal{Q}_i = \{q_i^j\}_{j=1}^{N_i}$ where $i \in \{p, c, a\}$, $q_i^j \in \mathbb{R}^d$ represents the j-th quantizer corresponding to the i-th attribute, with a hidden dimension d, and its codebook size of 1024. The number of quantizers for each attribute is $N_p = 1, N_c = 2, N_a = 3$. Thus, the output consists of a total of six sequences of discrete codes:

$$z = \textbf{Concat}(f_p(h), f_c(h), f_a(h)) \in \mathbb{R}^{T \times 6}, \tag{6}$$

where $f_p(h) \in \mathbb{R}^{T \times 1}$, $f_c(h) \in \mathbb{R}^{T \times 2}$, and $f_a(h) \in \mathbb{R}^{T \times 3}$ are functions that map the latent representation h into discrete codes representing the speech attributes, which are then concatenated into a unified representation z.

The timbre attribute is extracted by passing h through several Conformer blocks (Gulati et al., 2020) combined with a temporal pooling layer, which converts h into a timbre-specific representation:

$$z_t = \textbf{TemporalPooling}(\textbf{Conformer}(h)) \in \mathbb{R}^D. \tag{7}$$

After obtaining z and z_t, the neural codec decoder f_{dec} combines them to reconstruct the waveform:

$$y = f_{dec}(z, z_t). \tag{8}$$

Inspired by Eq. (8), which takes z and z_t as inputs and is pre-trained on a large-scale, multi-speaker dataset, ensuring robust zero-shot TTS capabilities, our approach aims to build a system that generates a six-sequence representation $\tilde{z} \in \mathbb{R}^{T \times 6}$, which is forced to lie within the subspaces of the pre-trained FACodec. This representation captures prosody, content, and acoustic details in a manner consistent with z. Subsequently, $\tilde{z}$ is fed into f_{dec}, alongside z_t, obtained using Eq. (7), to synthesize the speech output $\tilde{y}$.

A.2 Flow Matching

We present the fundamental principles of Flow Matching (FM) upon which our model is built. FM aims to construct a probability path $x_t \sim p_t(x)$, from a known source distribution $x_0 \sim p_0(x)$ (typically a Gaussian distribution) to a target distribution $x_1 \sim p_1(x)$. Specifically, FM is formulated as a regression objective for training a velocity field (also called a vector field), which models the instantaneous velocities of samples at time t (also known as the flow). This velocity field is then used to transform the source distribution p_0 into the target distribution p_1 along the probability path p_t. Formally, the flow of x along the trajectory is defined by an ordinary differential equation (ODE):

$$\frac{d}{dt} d\psi_t(x) = \mathbf{v}_t(\psi_t(x); \theta), \quad \psi_0(x) = x, \tag{9}$$

where $t \sim \mathcal{U}[0,1]$, $\psi_t : [0,1] \times \mathbb{R}^d \to \mathbb{R}^d$ represents a time-dependent flow describing the position of the point x at time t, and $\mathbf{v}_t : [0,1] \times \mathbb{R}^d \to \mathbb{R}^d$ is the time-dependent velocity field modeled by a neural network with parameters θ. Given $x_t := \psi_t(x_0)$, the velocity field $\mathbf{v}_t$ creates a probability path p_t such that $x_t \sim p_t$ for $x_0 \sim p_0$. Under this formulation, the objective is to regress velocity field $\mathbf{v}_t$ predicted by the neural network parameterized by θ to a target velocity field $\mathbf{u}_t$ in order to generate the desired probability path p_t. This is achieved by minimizing the Flow Matching (FM) loss:

$$\mathcal{L}_{FM}(\theta) = \mathbb{E}_{t,x_t}\left\|\mathbf{v}_t(x_t;\theta) - \mathbf{u}_t(x_t)\right\|^2, \quad (10)$$

where $t \sim \mathcal{U}[0,1],\ x_t \sim p_t$.

In practice, $\mathcal{L}_{FM}(\theta)$ is rarely implemented due to the complexity of $\mathbf{u}_t$ and the lack of prior knowledge of p_t, $\mathbf{u}_t$, and the target distribution p_1, which makes it an obstacle to directly calculate $\mathbf{u}_t(x_t)$. A feasible approach to address this issue is to simplify the loss by constructing the probability path p_t conditioned on real data x_1 from the training dataset. This path is also known as *conditional optimal transport* path. Following (Lipman et al., 2023), a random variable $x_t \sim p_t$ can be expressed as a linear combination of $x_0 \sim \mathcal{N}(x|0,I)$ and $x_1 \sim p_1$:

$$x_t = tx_1 + (1-t)x_0 \sim p_t, \quad (11)$$

Thus, the probability path $p_t(x|x_1) = \mathcal{N}(x|tx_1, (1-t)^2 I)$. Given x_t represents conditional random variables, the conditional velocity field can be derived from $\frac{d}{dt}x_t = \mathbf{u}_t(x_t|x_1)$ as $\mathbf{u}_t(x_t|x_1) = x_1 - x_0$. Using this, we can formulate a tractable and simplified version of the Flow Matching loss (10), referred to as the Conditional Flow Matching (CFM) loss. This formulation encourages straighter trajectories between the source and target distributions and is expressed as follows:

$$\begin{aligned}\mathcal{L}_{CFM}(\theta) &= \mathbb{E}_{t,x_0,x_1}\left\|\mathbf{v}_t(x_t;\theta) - \mathbf{u}_t(x_t|x_1)\right\|^2 \\ &= \mathbb{E}_{t,x_0,x_1}\left\|\mathbf{v}_t(x_t;\theta) - (x_1 - x_0)\right\|^2,\end{aligned} \quad (12)$$

where $t \sim \mathcal{U}[0,1],\ x_0 \sim \mathcal{N}(x|0,I),\ x_1 \sim p_1$. Once the training of the vector field $\mathbf{v}_t$ is complete, solving the ODE (9) at discretized time steps until $t = 1$ allows us to generate novel samples x_1 that approximate the target distribution p_1.

B Method Details

Prompting Trick during Training. As outlined in Section 3.3, incorporating an acoustic prompt is essential for generating $\mathbf{x}_1$. This process involves transferring prosody and acoustic detail attributes from the prompt to the output quantizers. A significant challenge arises in preparing prompt-target pairs that exhibit similar attributes, as mismatches can lead to degraded performance. To address this issue, we leverage ground truth quantizers, utilizing them as both the prompt and the target during training. Specifically, we randomly select and clone a segment of $1 \sim 3$ seconds from the ground truth data to serve as the prompt at each training step. This approach ensures a high degree of similarity between the prompt and target, facilitating more effective attribute transfer and enhancing the quality of the generated output.

Losses Computing Strategy. Let the velocity of $\breve{\mathbf{z}}_{\text{pr}}$ along the path progressing toward the corresponding $\mathbf{z}_1$ be represented as $\mathbf{v}_\theta^{1:L}(\breve{\mathbf{z}}_{\text{pr}}, \tau)$, where L denotes the length of the entire output sequence of $\mathbf{v}_\theta(\cdot,\cdot)$. Our goal is to compute the drift of $\mathbf{x}_{\text{pr}}$ for generating $\mathbf{x}_1$ only; it is unnecessary to backpropagate gradients over the entire output sequence, which includes the concatenation of acoustic prompt $\mathbf{y}$ and $\mathbf{x}_{\text{prior}}$ velocities. To address this, $\mathbf{v}_\theta^{1:L}(\breve{\mathbf{z}}_{\text{pr}}, \tau)$ is truncated by excluding the velocity components associated with the acoustic prompt $\mathbf{y}$, where M denotes its length. The resulting truncated velocity, $\mathbf{v}_\theta^{M:L}(\breve{\mathbf{z}}_{\text{pr}}, \tau)$, is then used in subsequent operations, including loss computation, to ensure computational efficiency while maintaining the focus on the target velocity for $\mathbf{x}_{\text{pr}}$. As a result, Eq. ((3)) is rewritten as:

$$\mathcal{L}_{CFM}(\theta) = \mathbb{E}_{\mathbf{x}_1,\mathbf{x}_{\text{pr}}}\left\|\mathbf{v}_\theta^{M:L}(\breve{\mathbf{z}}_{\text{pr}}, \tau) - \frac{\mathbf{x}_1 - \mathbf{x}_{\text{pr}}}{1-\tau}\right\|^2. \quad (13)$$

Consequently, the Anchor Loss $\mathcal{L}_{anchor}$ approximating the target distribution $\mathbf{x}_1$, conditioned on the $\tilde{\mathbf{x}}_1$ is formulated:

$$\mathcal{L}_{anchor}(\phi) = \mathbb{E}_{\mathbf{x}_1,\tilde{\mathbf{x}}_1}\left[-\log p(\mathbf{x}_1 \mid \tilde{\mathbf{x}}_1;\phi)\right], \quad (14)$$

where, $\tilde{\mathbf{x}}_1$ is computed as follows:

$$\tilde{\mathbf{x}}_1 = \mathbf{x}_{\text{pr}} + (1-\tau)\mathcal{F}^{-1}(\mathbf{v}_{\theta,M:L}(\breve{\mathbf{z}}_{\text{pr}}, \tau)).$$

C Training Details

We integrate the Prior Codes Generator and the Vector Field Estimator, exploring various configurations to optimize overall system performance.

For the Prior Codes Generator, we employ a compact neural network architecture with the following specifications: a hidden dimension of $d_{\text{model}} = 256$, a multi-head attention mechanism with $n_{\text{heads}} = 4$, and a feed forward network filter size of $d_{\text{ffn}} = 1024$. These parameters are consistently applied across both the encoder and decoder layers. The architecture includes 2 FFT blocks in both the encoder and the shared decoder, while an additional 6 blocks are utilized as specific layers to estimate the corresponding quantizers. The output dimensionality of the Prior Codes Generator is set to $\mathbf{x}_{\text{pr}} = 1024$, ensuring alignment with subsequent processing stages. For the Vector Field Estimator, we adopt a Transformer architecture comprising four layers, each characterized by a hidden dimension of $d_{\text{modlel}} = 1024$, a number of attention heads $n_{\text{heads}} = 32$, and a feedforward network inner dimension of $d_{\text{ffn}} = 4096$ for the base-size model.

The Prior Codes Generator and the Vector Field Estimator are jointly trained on a cluster of four 80GB A100 GPUs, using a batch size of 16. The training process employs the *AdamW* optimizer with a learning rate of 10^{-4}, $\beta_1 = 0.9$, $\beta_2 = 0.98$, and a weight decay parameter of 10^{-4}.

D Evaluation Details

D.1 Dataset Details

Training dataset. We use a subset of 500 hours from the *LibriTTS* dataset, where the duration of individual audio ranges from 1.0 to 16.6 seconds. From this dataset, we construct metadata for each training sample, which includes the following elements: input phonemes, target durations, and target code sequences. To derive the input phonemes and their corresponding target durations, we use the Montreal Forced Alignment (MFA) (McAuliffe et al., 2017) tool. This tool aligns each audio sample with its transcription and extracts the duration of each phoneme. Furthermore, we produce target codes using FACodec, which processes input waveforms sampled at 16 kHz. The FACodec applies a folding operation at a compression factor of 200. As a result, each second of audio is decomposed into a set of six quantizers, with each quantizer comprising 80 discrete speech units. These units have a value range spanning from 0 to 1023.

Evaluation dataset. We follow the VALL-E evaluation protocol (Chen et al., 2025). Particularly, the LibriSpeech test-clean dataset is filtered to include samples between 4 and 10 seconds in length, totaling 2.2 hours of audio. For each sample, the prompt speech is randomly selected from another sample by extracting a 1-second, 3-second, or 5-second clip, depending on the prompt setting used in our experiment, from the same speaker.

D.2 Metrics Details

We evaluate each system using the following objective evaluation metrics:

- **RTF** (Real-Time Factor) is an essential metric for assessing a system's efficiency, particularly in scenarios demanding real-time processing. It represents the time required to produce one second of speech. We assess the RTF of all models in a fully end-to-end setup using an NVIDIA 80GB A100 GPU.

- **NFE** (Number of Function Evaluations) denotes the total number of times the model's guiding function—often a score or drift function—is computed during the sampling process. This metric is especially important in settings where the generative process is formulated as solving an ordinary differential equation (ODE), such as in the probability flow ODE method used in score-based generative models.

- **UTMOS** (Saeki et al., 2022) is a deep learning-based system used to evaluate speech quality by predicting the mean opinion scores (MOS). It eliminates the need for costly, time-consuming subjective evaluations by using advanced deep learning techniques to provide predictions that closely align with human judgments.

- **SIM-O** and **SIM-R** are metrics used to evaluate speaker similarity. **SIM-O** measures the similarity between the synthesized speech and the original prompt, while **SIM-R** evaluates the similarity between the synthesized speech and the reconstructed prompt generated by FACodec (Ju et al., 2024b). These metrics are computed by calculating the cosine similarity of speaker embeddings extracted by applying WavLM-TDCNN [2] on the audio waveforms. Both SIM-O and SIM-R range from -1 to 1, with higher values indicating greater speaker similarity.

[2] https://github.com/microsoft/UniSpeech/tree/main/downstreams/speaker_verification

Table 5: Comparison of two OZSpeech model sizes: Base (145M parameters) and Small (100M parameters), evaluated on the *LibriSpeech test-clean* dataset. Both models were trained on the 500-hour *LibriTTS* training dataset.

			SPK-SIM		F0		Energy	
Model Size	**UTMOS (↑)**	**WER (↓)**	**SIM-O (↑)**	**SIM-R (↑)**	**Accuracy (↑)**	**RMSE (↓)**	**Accuracy (↑)**	**RMSE (↓)**
				1s Prompt				
Base	**3.17**	0.05	**0.30**	0.33	0.62	27.70	0.49	0.02
Small	3.15	0.05	0.29	0.33	**0.69**	**23.94**	**0.51**	0.02
				3s Prompt				
Base	**3.15**	**0.05**	**0.40**	**0.47**	**0.81**	**11.96**	**0.67**	0.01
Small	3.14	0.06	0.37	0.44	0.78	13.54	0.65	0.01
				5s Prompt				
Base	3.15	0.05	**0.39**	**0.48**	**0.83**	**12.05**	**0.67**	0.01
Small	**3.17**	0.05	0.38	0.46	0.79	12.58	0.66	0.01

- **WER** (Word Error Rate) is used to evaluate the robustness of speech synthesis systems, specifically how accurately they pronounce each word. We employ an ASR model [3] to transcribe the generated speech and compare the transcription with the text prompt. The ASR model used is a CTC-based HuBERT, pre-trained on LibriLight and fine-tuned on the 960-hour training set of LibriSpeech.

- **Prosody Accuracy & Error** are used to assess the alignment between the synthesized speech and audio prompt, with a specific focus on pitch (F0) and energy. For accuracy assessment, we adopt the methodology proposed in PromptTTS (Guo et al., 2022) and TextrolSpeech (Ji et al., 2024b), categorizing the F0 and energy levels of speech into three categories—high, normal, and low—based on their mean values [4]. Additionally, we employ the Root Mean Square Error (RMSE) to quantify the differences in F0 and energy between the synthesized speech and the corresponding prompts.

D.3 Baselines Details

We compare our model with previous zero-shot TTS baselines, including:

- **VoiceCraft** (Peng et al., 2024). We use the official code and pre-trained checkpoint [5], which is trained on the GigaSpeech dataset (Chen et al., 2021).

- **NaturalSpeech 2** (Shen et al., 2024). We use the Amphion toolkit (Zhang et al., 2024b) and pre-trained checkpoint [6], which is trained on the LibriTTS dataset (Zen et al., 2019).

- **F5-TTS** (Chen et al., 2024c). We use the official code and pre-trained checkpoint [7], which is trained on the Emilia dataset (He et al., 2024).

- **VALL-E** (Chen et al., 2025). We reproduce VALL-E using the Amphion toolkit (Zhang et al., 2024b) and train it under identical settings to our training dataset configuration.

E Extra Experiments

Table 5 shows the performance of OZSpeech-Base (145M parameters) and OZSpeech-Small (100M parameters). Although at over 31% reduction in size, the Small model shows comparable performance with the Base model across all metrics, except for pitch (**F0**). Interestingly, the Small model outperforms the Base model by 13.6% in F0 RMSE for 1s prompt length (23.94 for Small vs. 27.70 for Base). However, for 3s prompt length, it experiences a 13.2% relative decline in the same metric (13.54 for Small vs. 11.96 for Base).

F Analysis

As shown in Figure 2, the distributions of performance metrics across different prompt lengths are as follows:

[3] https://huggingface.co/facebook/hubert-large-ls960-ft

[4] https://github.com/jishengpeng/TextrolSpeech

[5] https://huggingface.co/pyp1/VoiceCraft/blob/main/830M_TTSEnhanced.pth

[6] https://huggingface.co/amphion/naturalspeech2_libritts/tree/main/checkpoint

[7] https://huggingface.co/SWivid/F5-TTS/blob/main/F5TTS_Base_bigvgan/model_1250000.pt

- **WER**: For the 1s prompt, OZSpeech exhibits a distribution that is very close to zero with a narrow box, indicating superior performance. The second best is NaturalSpeech 2, which shows a slightly right-shifted box compared to OZSpeech, followed by VoiceCraft. This pattern is consistent across the 3s and 5s prompts. In contrast, VALL-E and F5-TTS display higher distributions. Notably, F5-TTS shows slightly better performance than VALL-E for the 1s prompt. However, as the prompt length increases, F5-TTS significantly lags behind the other baselines, with its distribution approaching 0.5.

- **UTMOS**: The best performance for this metric is achieved by VALL-E for the 1s prompt. Its distribution shifts slightly to the right for the 3s prompt and stabilizes for the 5s prompt. VoiceCraft and OZSpeech show the next best performances, maintaining stable distributions across different prompt lengths, with VoiceCraft consistently outperforming OZSpeech. NaturalSpeech 2 scores mostly below 3.0 for the 1s prompt and shows improvement as the prompt length increases. Notably, F5-TTS consistently scores below 1.5, significantly lagging behind the other baselines.

- **SIM-O**: For the 1s prompt, the distributions of VoiceCraft and OZSpeech are almost equivalent, followed by VALL-E, F5-TTS, and NaturalSpeech 2, respectively. As the prompt length increases, the differences among the models become more noticeable. Specifically, VoiceCraft shows the best performance in retaining the speaker's identity in the synthesized output. VALL-E follows with the second-best performance, followed by OZSpeech and NaturalSpeech 2, respectively. In contrast, F5-TTS consistently demonstrates poor performance regardless of the prompt length.

All in all, OZSpeech achieved competitive performance compared to other baselines. Although our method does not show a clear performance advantage over baseline models, our primary objective is to balance sampling speed and speech synthesis capability. This trade-off enables our method to maintain a small model size with low WER while preserving the naturalness of the speech and the speaker's identity style from the prompt in the synthesized output. In contrast to the baselines, which have larger models and require longer inference times (see Table 2), our method demonstrates a significant advantage. With just one sampling step, we can achieve promising performance.

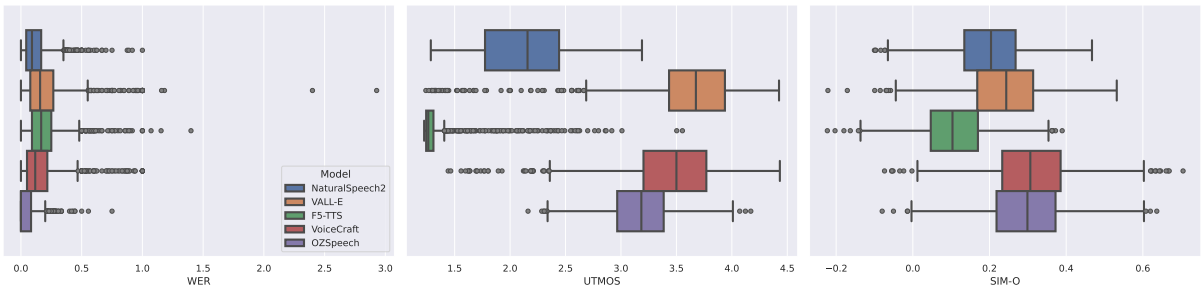

(a) 1s Prompt

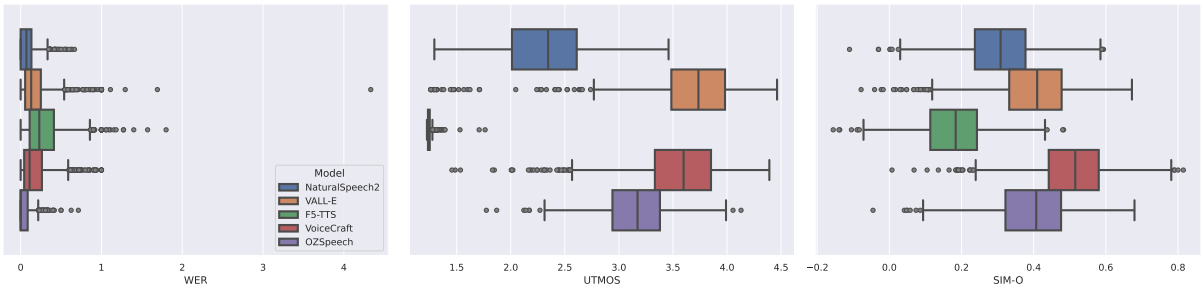

(b) 3s Prompt

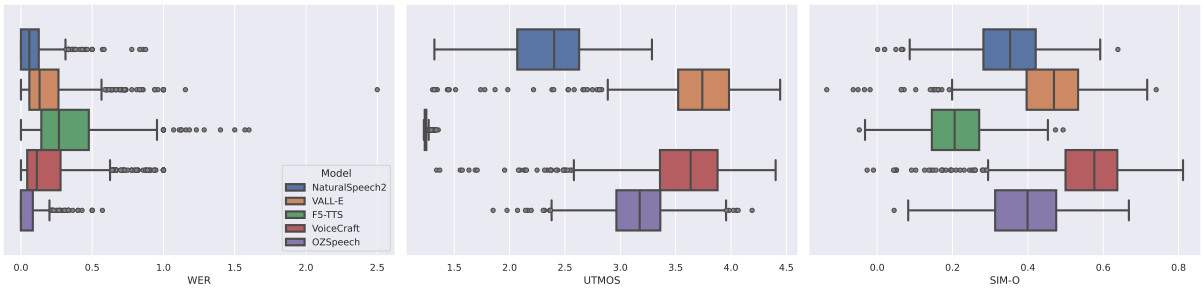

(c) 5s Prompt

Figure 2: Boxplots showing the distributions of performance metrics (WER, UTMOS, and SIM-O) on the LibriSpeech test-clean dataset for each model, evaluated across different audio prompt lengths.